A numerical Green's function boundary element approach for an anti-plane dynamic piezoelectric crack problem

W. T. Ang[1]* and L. Athanasius[2]

[1]*School of Mechanical and Aerospace Engineering, Nanyang Technological University, Singapore 639798*
e-mail: mwtang@ntu.edu.sg

[2]*School of Mechanical and Aerospace Engineering, Nanyang Technological University,Singapore 639798*
e-mail: atha0001@e.ntu.edu.sg

Abstract

An anti-plane electro-elastic dynamic problem involving a stress-free and electrically impermeable planar crack in a piezoelectric body is considered. In the Laplace transform domain, Green's functions satisfying appropriate conditions on the crack are constructed numerically by using the hyper-singular integral method. They are then used to obtain a boundary element method for solving the crack problem in the Laplace transform domain. Discretization of the crack faces into elements is not required. The relevant crack tip stress and electrical displacement intensity factors in the Laplace transform domain can be computed easily and inverted numerically to obtain the corresponding intensity factors in the physical time domain. For a special case of the problem, the boundary element solution is verified using a semi-analytic Fourier integral transform solution.

Keywords: dynamic crack problem, electro-elasticity, piezoelectric material, Green's function, boundary element

1. Introduction

The Green's function boundary integral method for solving elasto-static crack problems is well established (see [2], [3], [6] and [8]). Green's functions satisfying relevant boundary conditions on the crack faces may be derived to develop boundary element procedures that do not require the crack faces to be discretized into elements. The Green's functions give highly accurate numerical procedures for computing the crack tip stress intensity factors. They are, however, difficult to obtain in analytic closed-form for cracks with arbitrary geometries, configurations and boundary conditions.

To solve a wider range of crack problems, Telles et al. [10] constructed numerically the required Green's functions by the hyper-singular integral method. This approach was extended by Ang and Telles [4] to solve a static problem involving multiple interacting planar cracks in an anisotropic body. More recently, Athanasius et al. [5] derived numerical Green's functions for planar cracks in piezoelectric solids under static loading.

The numerical Green's function approach is further developed here to solve an anti-plane electro-elastic dynamic problem involving a stress-free and electrically impermeable planar crack in a piezoelectric body. In the Laplace transform domain, Green's functions satisfying appropriate conditions on the crack faces are constructed numerically and employed to obtain a boundary element method to solve the problem. Once the problem is solved, the crack tip stress and electrical displacement intensity factors in the Laplace transform domain can be extracted easily and inverted numerically to the corresponding intensity factors in the physical time domain. For a specific case of the problem in which the crack lies in the center of a square domain having dimensions that are very large compared to the length of the crack, the stress intensity factor computed is found to be in good agreement with the one calculated from a semi-analytic Fourier integral transform solution. Dynamic crack tip stress and electrical displacement intensity factors are also calculated for another specific case involving a rectangular piezoelectric domain with electroded parts of the boundary.

2. The problem

With reference to a Cartesian coordinate frame $Ox_1x_2x_3$ consider a homogeneous piezoelectric solid whose geometry does not change along the x_3 axis. The interior of the solid contains a planar crack in the region $-a < x_1 < a,\ x_2 = 0, -\infty < x_3 < \infty$. As shown in Fig. 1, on the Ox_1x_2 plane, the interior of the solid is given by R, the exterior boundary by the simple closed curve C and the crack appears as a straight horizontal cut of length $2a$ on the x_1 axis.

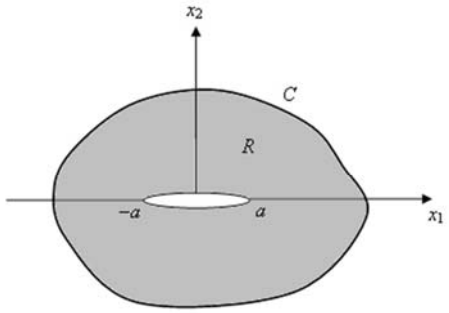

Figure 1: A geometrical sketch of the problem

The piezoelectric solid undergoes an anti-plane deformation. Specifically, its electrical poling is along the x_3 axis, its displacement is such that its x_3 component is the only non-zero component and the displacement and electrical potential are functions of x_1, x_2 and time only.

At each and every point on the exterior boundary C, either the displacement or the traction and either the electrical potential or the normal electrical displacement are suitably prescribed. The prescribed quantities are independent of x_3 but they may vary with time. The displacement and its first order partial derivative with respect to time are initially zero at all points inside the solid, that is, the solid is initially undeformed

*This work is supported by a Singapore Ministry of Education Tier 1 grant RG 9/09 awarded by Nanyang Technological University to the first author. The assistance given by Mrs. Gomathi M Ramesh in the early stage of this work is acknowledged.

and at rest. The crack is assumed to be stress-free and electrically impermeable.

The problem is to determine the displacement and the electrical potential throughout the solid. Of particular interest is the calculation of the dynamic crack tip stress and electrical displacement intensity factors.

3. Basic equations

The mechanical equilibrium equation and the electric Maxwell equation in the piezoelectric solid are given by

$$\frac{\partial \sigma_{3i}}{\partial x_i} = \rho \frac{\partial^2 u_3}{\partial t^2} \text{ and } \frac{\partial D_i}{\partial x_i} = 0, \tag{1}$$

where u_3 is the x_3 component of the displacement, σ_{3i} are the anti-plane stresses, D_i is the x_i component of the in-plane electrical displacement, ρ is the (mass) density of the solid and t denotes time. Note that in (1) summation is implied over the repeated subscript i running from 1 to 2.

The constitutive relations are

$$\sigma_{3i} = c_{44} \frac{\partial u_3}{\partial x_i} + e_{15} \frac{\partial \phi}{\partial x_i} \text{ and } D_i = e_{15} \frac{\partial u_3}{\partial x_i} - \varepsilon_{11} \frac{\partial \phi}{\partial x_i}, \tag{2}$$

where ϕ is the electrical potential and c_{44}, e_{15} and ε_{11} (all assumed constants here) are respectively the elastic shear modulus, the piezoelectric coefficient and the dielectric coefficient of the piezoelectric solid.

Use of (1) and (2) yields the governing partial differential equations

$$\frac{\partial^2 u_3}{\partial x_i \partial x_i} = \frac{1}{c^2} \frac{\partial^2 u_3}{\partial t^2} \text{ and } \frac{\partial^2}{\partial x_i \partial x_i}(e_{15}\, u_3 - \varepsilon_{11}\phi) = 0, \tag{3}$$

where $c = \sqrt{(\varepsilon_{11} c_{44} + e_{15}^2)/(\rho \varepsilon_{11})}$ is the speed of the shear wave.

With the introduction of the following non-dimensionalized variables

$$\begin{aligned}
&\bar{x}_i = \frac{x_i}{a}, \bar{t} = \frac{ct}{a}, \\
&\bar{u}_3(\bar{x}_1, \bar{x}_2, \bar{t}) = \frac{u_3\left(a\bar{x}_1, a\bar{x}_2, \frac{a\bar{t}}{c}\right)}{a}, \\
&\bar{\sigma}_{3i}(\bar{x}_1, \bar{x}_2, \bar{t}) = \frac{\sigma_{3i}\left(a\bar{x}_1, a\bar{x}_2, \frac{a\bar{t}}{c}\right)}{c_{44}}, \\
&\bar{\phi}(\bar{x}_1, \bar{x}_2, \bar{t}) = \frac{\varepsilon_{11}\phi\left(a\bar{x}_1, a\bar{x}_2, \frac{a\bar{t}}{c}\right)}{a e_{15}}, \\
&\bar{D}_i(\bar{x}_1, \bar{x}_2, \bar{t}) = \frac{D_i\left(a\bar{x}_1, a\bar{x}_2, \frac{a\bar{t}}{c}\right)}{e_{15}},
\end{aligned} \tag{4}$$

the constitutive relations in (2) can be re-written in non-dimensionalized form by

$$\bar{\sigma}_{3i} = \frac{\partial \bar{u}_3}{\partial \bar{x}_i} + \bar{e}_{15} \frac{\partial \bar{\phi}}{\partial \bar{x}_i} \text{ and } \bar{D}_i = \frac{\partial \bar{u}_3}{\partial \bar{x}_i} - \frac{\partial \bar{\phi}}{\partial \bar{x}_i}, \tag{5}$$

and the governing equations in (3) by

$$\frac{\partial^2 \bar{u}_3}{\partial \bar{x}_i \partial \bar{x}_i} = \frac{\partial^2 \bar{u}_3}{\partial \bar{t}^2} \text{ and } \frac{\partial^2}{\partial \bar{x}_i \partial \bar{x}_i}(\bar{u}_3 - \bar{\phi}) = 0, \tag{6}$$

where $\bar{e}_{15} = e_{15}^2/(c_{44}\varepsilon_{11})$.

Henceforth, the analysis presented here deals with only non-dimensionalized variables. For convenience, the overhead bar used to denote non-dimensionalized variables will be omitted. Thus, for example, $\bar{x}_i$ and $\bar{\sigma}_{3i}$ will be written as simply x_i and σ_{3i} respectively.

4. Formulation in Laplace transform space

Application of the Laplace transform (with respect to the non-dimensionalized time $t \geq 0$) on (6) yields

$$\frac{\partial^2 u_3^*}{\partial x_i \partial x_i} - s^2 u_3^* = 0 \text{ and } \frac{\partial^2}{\partial x_i \partial x_i}(u_3^* - \phi^*) = 0, \tag{7}$$

where s is the Laplace transform parameter (assumed real here) and * denotes the Laplace transform of the function, that is, the Laplace transform of the function $f(x_1, x_2, t)$ is $f^*(x_1, x_2, s)$ defined by

$$f^*(x_1, x_2, s) = \int_0^\infty f(x_1, x_2, t) \exp(-st)\, dt. \tag{8}$$

In the Laplace transform space, the problem is to solve (7) in the piezoelectric solid subject to prescribed values of either u_3^* or p_3^* (the Laplace transform of the non-dimensionalized anti-plane traction) and either ϕ^* or d^* (the Laplace transform of the non-dimensionalized normal electrical displacement) at each and every point on the exterior boundary C and the conditions on the crack as given by

$$\lim_{x_2 \to 0} \sigma_{32}^*(x_1, x_2, s) = 0 \text{ and } \lim_{x_2 \to 0} D_2^*(x_1, x_2, s) = 0 \quad \text{for } -1 < x_1 < 1. \tag{9}$$

Note that the functions p_3^* and d^* are respectively defined by $p_3^*(x_1, x_2, s) = \sigma_{3i}^*(x_1, x_2, s) n_i(x_1, x_2)$ and $d^*(x_1, x_2, s) = D_i^*(x_1, x_2, s) n_i(x_1, x_2)$, where $[n_1(x_1, x_2), n_2(x_1, x_2)]$ is the outward unit normal vector to C at the point (x_1, x_2).

5. Boundary integral equations

The governing partial differential equations in (7) may be re-cast into boundary integral equations given by

$$\begin{aligned}
\lambda(\xi_1, \xi_2) u_3^*(\xi_1, \xi_2, s) = \int_C \{ & u_3^*(x_1, x_2, s)\, \Gamma(x_1, x_2, \xi_1, \xi_2, s) \\
& - [\alpha p_3^*(x_1, x_2, s) + \beta d^*(x_1, x_2, s)] \\
& \times \Psi(x_1, x_2, \xi_1, \xi_2, s)\} dS(x_1, x_2),
\end{aligned} \tag{10}$$

and

$$\begin{aligned}
&\lambda(\xi_1, \xi_2)[u_3^*(\xi_1, \xi_2, s) - \phi^*(\xi_1, \xi_2, s)] \\
&= \int_C \{[u_3^*(x_1, x_2, s) - \phi^*(x_1, x_2, s)] \Lambda(x_1, x_2, \xi_1, \xi_2) \\
&\quad - d^*(x_1, x_2, s) \Phi(x_1, x_2, \xi_1, \xi_2)\} dS(x_1, x_2),
\end{aligned} \tag{11}$$

where $\alpha = e_{15}^{-1}\beta = 1/(1+e_{15})$, $\lambda(\xi_1,\xi_2) = 1$ if (ξ_1,ξ_2) lies in the interior of the solution domain, $\lambda(\xi_1,\xi_2) = 1/2$ if (ξ_1,ξ_2) lies on a smooth part of C and the Green's functions Ψ and Φ are given by

$$\Psi(x_1,x_2,\xi_1,\xi_2,s) = -\frac{1}{2\pi}K_0\big(sr(x_1,x_2,\xi_1,\xi_2)\big) + \Psi_0(x_1,x_2,\xi_1,\xi_2,s),$$

$$\Phi(x_1,x_2,\xi_1,\xi_2) = \frac{1}{2\pi}\ln\big(r(x_1,x_2,\xi_1,\xi_2)\big) + \Phi_0(x_1,x_2,\xi_1,\xi_2),$$

$$\Gamma(x_1,x_2,\xi_1,\xi_2,s) = n_i(x_1,x_2)\frac{\partial}{\partial x_i}[\Psi(x_1,x_2,\xi_1,\xi_2,s)],$$

$$\Lambda(x_1,x_2,\xi_1,\xi_2) = n_i(x_1,x_2)\frac{\partial}{\partial x_i}[\Phi(x_1,x_2,\xi_1,\xi_2)], \qquad (12)$$

where $r(x_1,x_2,\xi_1,\xi_2) = \sqrt{(x_1-\xi_1)^2+(x_2-\xi_2)^2}$, K_0 is the zero-th order modified Bessel function defined in [1] and Ψ_0 and Φ_0 are solutions of

$$\frac{\partial^2\Psi_0}{\partial x_i\partial x_i} - s^2\Psi_0 = 0 \text{ and } \frac{\partial^2\Phi_0}{\partial x_i\partial x_i} = 0, \qquad (13)$$

chosen to satisfy the conditions (on the crack) given by

$$\lim_{x_2\to 0}\frac{\partial\Psi_0}{\partial x_2} = \frac{s\xi_2K_1\big(sr(x_1,0,\xi_1,\xi_2)\big)}{2\pi r(x_1,0,\xi_1,\xi_2)} \text{ for } -1<x_1<1, \qquad (14)$$

and

$$\lim_{x_2\to 0}\frac{\partial\Phi_0}{\partial x_2} = \frac{\xi_2}{2\pi(r(x_1,0,\xi_1,\xi_2))^2} \text{ for } -1<x_1<1, \qquad (15)$$

with K_1 being the first order modified Bessel function.

Note that there is no integration over the crack faces in the boundary integral equations in (10) and (11) because of (14) and (15).

A numerical procedure for constructing the functions Ψ_0 and Φ_0 is given below.

6. Numerical Green's functions

Guided by the analysis in [4] and [5], for (x_1,x_2) and (ξ_1,ξ_2) in the interior of the Ox_1x_2 plane containing the crack $-1<x_1<1$, $x_2=0$, we take Ψ_0 and Φ_0 to be given by

$$\Psi_0(x_1,x_2,\xi_1,\xi_2,s) = \int_{-1}^{1}\frac{sx_2K_1\big(sr(y,0,x_1,x_2)\big)\Delta\Psi_0(y,\xi_1,\xi_2,s)}{2\pi r(y,0,x_1,x_2)}dy,$$

$$\Phi_0(x_1,x_2,\xi_1,\xi_2) = \int_{-1}^{1}\frac{x_2\Delta\Phi_0(y,\xi_1,\xi_2)}{2\pi[r(y,0,x_1,x_2)]^2}dy, \qquad (16)$$

where $\Delta\Psi_0(y,\xi_1,\xi_2,s)$ and $\Delta\Phi_0(y,\xi_1,\xi_2)$ respectively give the jumps of the functions $\Psi_0(x_1,x_2,\xi_1,\xi_2,s)$ and $\Phi_0(x_1,x_2,\xi_1,\xi_2)$ across the crack at the point $(x_1,x_2) = (y,0)$ $(-1<y<1)$.

Use of (16) in (14) and (15) yields the hyper-singular integral equations

$$\mathcal{K}\int_{-1}^{1}\frac{\Delta\Psi_0(y,\xi_1,\xi_2,s)}{(y-w)^2}dy + \mathcal{C}\int_{-1}^{1}\Delta\Psi_0(y,\xi_1,\xi_2,s)\Omega(y,w,s)dy = \frac{s\xi_2K_1\big(sr(w,0,\xi_1,\xi_2)\big)}{r(w,0,\xi_1,\xi_2)} \text{ for } -1<w<1, \qquad (17)$$

and

$$\mathcal{K}\int_{-1}^{1}\frac{\Delta\Phi_0(y,\xi_1,\xi_2)}{(y-w)^2}dy = \frac{\xi_2}{(r(w,0,\xi_1,\xi_2))^2} \text{ for } -1<w<1, \qquad (18)$$

where $\mathcal{K}$ and $\mathcal{C}$ denote integrals to be interpreted in the Hadamard finite-part and Cauchy principal sense respectively and

$$\Omega(y,w,s) = \frac{sK_1(s|y-w|)}{|y-w|} - \frac{1}{(y-w)^2}. \qquad (19)$$

To solve (17) and (18) for $\Delta\Psi_0$ and $\Delta\Phi_0$ using the collocation technique described in [7], we let

$$\Delta\Psi_0(y,\xi_1,\xi_2,s) \cong \sqrt{1-y^2}\sum_{j=1}^{J}\psi_j(\xi_1,\xi_2,s)U_{j-1}(y),$$

$$\Delta\Phi_0(y,\xi_1,\xi_2) \cong \sqrt{1-y^2}\sum_{j=1}^{J}\mu_j(\xi_1,\xi_2)U_{j-1}(y), \qquad (20)$$

where $U_j(y)$ $(-1<y<1)$ is the j-th order Chebyshev polynomial of the second kind and ψ_j and μ_j are coefficients yet to be determined.

Substituting (20) into (17) and (18) and collocating at $w = w_i \equiv \cos((2i-1)\pi(2J)^{-1})$ for $i = 1,2,\dots,J$, we obtain

$$\sum_{j=1}^{J}\psi_j(\xi_1,\xi_2,s)[-j\pi\,U_{j-1}(w_i) + \Xi_j(w_i,s)] = \frac{s\xi_2K_1\big(sr(w_i,0,\xi_1,\xi_2)\big)}{r(w_i,0,\xi_1,\xi_2)} \text{ for } i = 1,2,\dots,J, \qquad (21)$$

and

$$-\sum_{j=1}^{J}j\pi\mu_j(\xi_1,\xi_2)U_{j-1}(w_i) = \frac{\xi_2}{(r(w_i,0,\xi_1,\xi_2))^2} \text{ for } i = 1,2,\dots,J, \qquad (22)$$

where

$$\Xi_j(w,s) = \mathcal{C}\int_{-1}^{1}\sqrt{1-y^2}\Omega(y,w,s)U_{j-1}(y)dy. \qquad (23)$$

We can easily invert (21) and (22) as systems of linear algebraic equations to obtain ψ_j and μ_j. The Green's functions Ψ and Φ in (12) can then be evaluated using

$$\Psi(x_1,x_2,\xi_1,\xi_2,s) = -\frac{1}{2\pi}K_0\big(sr(x_1,x_2,\xi_1,\xi_2)\big)$$

$$+\sum_{j=1}^{J} sx_2\,\psi_j(\xi_1,\xi_2,s)\int_{-1}^{1}\frac{K_1\big(sr(y,0,x_1,x_2)\big)U_{j-1}(y)\sqrt{1-y^2}}{2\pi r(y,0,x_1,x_2)}dy,$$

$$\Phi(x_1,x_2,\xi_1,\xi_2) = \frac{1}{2\pi}\ln\big(r(x_1,x_2,\xi_1,\xi_2)\big)$$

$$+\sum_{j=1}^{J} x_2\,\mu_j(\xi_1,\xi_2)\int_{-1}^{1}\frac{\sqrt{1-y^2}\,U_{j-1}(y)}{2\pi[r(y,0,x_1,x_2)]^2}dy. \qquad (24)$$

The integrands in the integrals in (24) are well-defined over $-1 < y < 1$ for points (x_1, x_2) that are not on the crack. Hence, for the evaluation of the Green's functions Ψ and Φ in the boundary integrals of (12), the integrals in (24) can be easily and accurately evaluated by using a suitable numerical integration formula in [1] (as explained in [4], [5], [7] and [10]).

7. Boundary element method

The exterior boundary C is discretized into M straight elements denoted by $C^{(k)}$ $(k = 1, 2, \dots, M)$. We assume that $u_3^*(x_1,x_2,s)$, $\phi^*(x_1,x_2,s)$, $p_3^*(x_1,x_2,s)$ and $d^*(x_1,x_2,s)$ do not vary spatially over $C^{(k)}$ and are approximately given by $u^{(k)}(s)$, $\phi^{(k)}(s)$, $p^{(k)}(s)$ and $d^{(k)}(s)$ respectively.

The boundary integral equations in (10) and (11) may be approximated as

$$\frac{1}{2}u^{(j)}(s) = \sum_{k=1}^{M}\{\,u^{(k)}(s)\int_{C^{(k)}}\Gamma\left(x_1,x_2,y_1^{(j)},y_2^{(j)},s\right)dS(x_1,x_2)$$

$$-[\alpha p^{(k)}(s)+\beta d^{(k)}(s)]$$

$$\times\int_{C^{(k)}}\Psi\left(x_1,x_2,y_1^{(j)},y_2^{(j)},s\right)dS(x_1,x_2)\}$$

$$\text{for } j = 1,2,\dots,M, \qquad (25)$$

and

$$\frac{1}{2}[u^{(j)}(s)-\phi^{(j)}(s)] = \sum_{k=1}^{M}\{\,[u^{(k)}(s)-\phi^{(k)}(s)]$$

$$\times\int_{C^{(k)}}\Lambda\left(x_1,x_2,y_1^{(j)},y_2^{(j)}\right)dS(x_1,x_2)$$

$$-d^{(k)}(s)\int_{C^{(k)}}\Phi\left(x_1,x_2,y_1^{(j)},y_2^{(j)}\right)dS(x_1,x_2)\}$$

$$\text{for } j = 1,2,\dots,M, \qquad (26)$$

where $(y_1^{(j)}, y_2^{(j)})$ is the midpoint of the element $C^{(j)}$.

There are $2M$ unknown functions of the Laplace transform parameter s in (25) and (26). Depending on the prescribed boundary conditions on the exterior boundary C, either $u^{(k)}(s)$ or $p^{(k)}(s)$ and either $\phi^{(k)}(s)$ or $d^{(k)}(s)$ are not known on $C^{(k)}$. We may solve (25) and (26) as a system of $2M$ linear algebraic equations for the $2M$ unknown functions of s. Once $u^{(k)}(s)$, $\phi^{(k)}(s)$, $p^{(k)}(s)$ and $d^{(k)}$ are all known, the crack tip stress and electric displacement intensity factors can be extracted as explained below.

8. Stress and electric displacement intensity factors

The (non-dimensionalized) stress and electric displacement intensity factors at the crack tip $(0, \pm 1)$, denoted by $K_{III}^{\pm}$ and $K_{IV}^{\pm}$ respectively, are defined by

$$K_{III}^{\pm}(t) = \lim_{x_1\to\pm 1^{\pm}}\sqrt{2(\pm x_1-1)}\;\sigma_{32}\,(x_1,0,t),$$

$$K_{IV}^{\pm}(t) = \lim_{x_1\to\pm 1^{\pm}}\sqrt{2(\pm x_1-1)}\;D_2\,(x_1,0,t). \qquad (27)$$

Following closely the analysis in [4], [5] and [10], in order to extract the intensity factors in the Laplace transform domain, we first solve for the jumps in $u_3^*(x_1,x_2,s)$ and $\phi^*(x_1,x_2,s)$ across the opposite crack faces by solving the hyper-singular integral equations

$$\frac{1}{2\pi}\mathcal{K}\int_{-1}^{1}\frac{\Delta u_3^*(y,s)}{(y-w)^2}dy + \frac{1}{2\pi}\mathcal{C}\int_{-1}^{1}\Delta u_3^*(y,s)\Omega(y,w,s)dy$$

$$= G(w,s) \text{ for } -1 < w < 1, \qquad (28)$$

and

$$\frac{1}{2\pi}\mathcal{K}\int_{-1}^{1}\frac{\Delta u_3^*(y,s)-\Delta\phi^*(y,s)}{(y-w)^2}dy$$

$$= F(w,s) \text{ for } -1 < w < 1, \qquad (29)$$

where $\Delta u_3^*(y,s)$ and $\Delta\phi^*(y,s)$ respectively give the jumps in $u_3^*(x_1,x_2,s)$ and $\phi^*(x_1,x_2,s)$ at the point $(x_1,x_2) = (y,0)$ on the crack and

$$G(w,s) = -\frac{1}{2\pi}\int_C\{\,u_3^*(x_1,x_2,s)L_1(x_1,x_2,w,s)$$

$$+[\alpha p_3^*(x_1,x_2,s)+\beta d^*(x_1,x_2,s)]L_2(x_1,x_2,w,s)\}dS(x_1,x_2),$$

$$F(w,s) = -\frac{1}{2\pi}\int_C\{\,[u_3^*(x_1,x_2,s)-\phi^*(x_1,x_2,s)]L_3(x_1,x_2,w)$$

$$+d^*(x_1,x_2,s)L_4(x_1,x_2,w)\}dS(x_1,x_2),$$

$$L_1(x_1,x_2,w,s) = s\{\frac{K_1(sr(x_1,x_2,w,0))}{(r(x_1,x_2,w,0))^3}$$

$$\times[n_1(x_1,x_2)x_2(x_1-w)-n_2(x_1,x_2)(x_1-w)^2]$$

$$-\frac{sx_2K_1'(sr(x_1,x_2,w,0))}{(r(x_1,x_2,w,0))^2}$$

$$\times[n_1(x_1,x_2)(x_1-w)+n_2(x_1,x_2)x_2]\},$$

$$L_2(x_1,x_2,w,s)=\frac{sx_2K_1(sr(x_1,x_2,w,0))}{r(x_1,x_2,w,0)},$$

$$L_3(x_1,x_2,w)=\frac{1}{(r(x_1,x_2,w,0))^4}\{2n_1(x_1,x_2)(x_1-w)x_2$$

$$+n_2(x_1,x_2)(x_2^2-(x_1-w)^2)\},$$

$$L_4(x_1,x_2,w)=\frac{x_2}{(r(x_1,x_2,w,0))^2}. \qquad (30)$$

Note that $G(w,s)$ and $F(w,s)$ in (30) may be interpreted as the Laplace transforms of the internal loads (stress and electrical displacement) on the crack.

To solve (28) and (29) approximately, let

$$\Delta u_3^*(y,s)\cong\sqrt{1-y^2}\sum_{j=1}^{J}\tau_j(s)U_{j-1}(y),$$

$$\Delta u_3^*(y,s)-\Delta\phi^*(y,s)\cong\sqrt{1-y^2}\sum_{j=1}^{J}\upsilon_j(s)U_{j-1}(y), \qquad (31)$$

where $\tau_j(s)$ and $\upsilon_j(s)$ are obtained by inverting

$$\frac{1}{2\pi}\sum_{j=1}^{J}\tau_j(s)[-j\pi\,U_{j-1}(w_i)+\Xi_j(w_i,s)]$$

$$=G(w_i,s)\ \text{ for }\ i=1,2,\dots,J, \qquad (32)$$

and

$$-\frac{1}{2}\sum_{j=1}^{J}j\upsilon_j(s)U_{j-1}(w_i)=G(w_i,s)\ \text{for}\ i=1,2,\dots,J. \qquad (33)$$

Note that $G(w,s)$ and $F(w,s)$ as given in (30) can be evaluated numerically by discretizing the boundary C into elements as described in the previous section and using the values of $u^{(k)}(s)$, $\phi^{(k)}(s)$, $p^{(k)}(s)$ and $d^{(k)}(s)$ obtained from (25) and (26).

If $\tilde{k}_{III}^{\pm}(s)$ and $\tilde{k}_{IV}^{\pm}(s)$ are the Laplace transform of $K_{III}^{\pm}(t)$ and $K_{IV}^{\pm}(t)$ respectively then (see [7])

$$\tilde{k}_{III}^{\pm}(s)=\frac{1}{2}\sum_{j=1}^{J}\{(1+e_{15})\,\tau_j(s)-e_{15}\upsilon_j(s)\}U_{j-1}(\pm1),$$

$$\tilde{k}_{IV}^{\pm}(s)=\frac{1}{2}\sum_{j=1}^{J}\upsilon_j(s)U_{j-1}(\pm1). \qquad (34)$$

The Stehfest's algorithm [9] may be used to recover $K_{III}^{\pm}(t)$ and $K_{IV}^{\pm}(t)$ from (34) as follows:

$$K_{III}^{\pm}(t)\cong\frac{\ln(2)}{t}\sum_{n=1}^{2P}g_n\tilde{k}_{III}^{\pm}\left(\frac{n\ln(2)}{t}\right),$$

$$K_{IV}^{\pm}(t)\cong\frac{\ln(2)}{t}\sum_{n=1}^{2P}g_n\tilde{k}_{IV}^{\pm}\left(\frac{n\ln(2)}{t}\right),$$

$$g_n=(-1)^{n+P}\sum_{m=\left[\frac{n+1}{2}\right]}^{\min(n,P)}\frac{m^P\hat{g}_{nm}}{(P-m)!},$$

$$\hat{g}_{nm}=\frac{(2m)!}{m!\,(m-1)!\,(n-m)!\,(2m-n)!}, \qquad (35)$$

where $[(n+1)/2]$ denotes the integer part of $(n+1)/2$.

9. A semi-analytic Fourier transform solution

For a particular case of the piezoelectric crack problem under consideration, take the electrically impermeable crack $-1<x_1<1$, $x_2=0$, to be in the square domain $-\ell<x_1<\ell$, $-\ell<x_2<\ell$, where ℓ is a given positive constant such that $\ell>1$. The boundary conditions on the sides of the square domain are taken to be given by

$$\left.\begin{matrix}\sigma_{32}(x_1,\pm\ell,t)=H(t)\\ D_2(x_1,\pm\ell,t)=H(t)\end{matrix}\right\}\ \text{for}\ -\ell<x_1<\ell,$$

$$\left.\begin{matrix}\sigma_{31}(\pm\ell,x_2,t)=0\\ D_1(\pm\ell,x_2,t)=0\end{matrix}\right\}\ \text{for}\ -\ell<x_2<\ell. \qquad (36)$$

For $\ell>>1$, the Fourier integral transformation may be used to derive a semi-analytic solution for the problem in the Laplace transform domain as follows.

Let u_3^* and ϕ^* be given by

$$u_3^*(x_1,x_2,s)=\frac{\sinh(sx_2)}{s^2\cosh(s\ell)}+v(x_1,x_2,s),$$

$$\phi^*(x_1,x_2,s)=-\frac{x_2}{s}+\frac{\sinh(sx_2)}{s^2\cosh(s\ell)}+\varphi(x_1,x_2,s). \qquad (37)$$

For any $\ell>1$, the boundary conditions in (36) are exactly satisfied if we take $v(x_1,x_2,s)=0$ and $\varphi(x_1,x_2,s)=0$. For $\ell>>1$ (that is, for the case in which the size of the square domain is very much larger than the length of the centrally located crack), if $v(x_1,x_2,s)$ and $\varphi(x_1,x_2,s)$ have negligible effects on the electro-elastic fields at large distance from the crack then the functions $v(x_1,x_2,s)$ and $\varphi(x_1,x_2,s)$ are solutions of

$$\frac{\partial^2 v}{\partial x_i\partial x_i}-s^2v=0\ \text{ and }\ \frac{\partial^2}{\partial x_i\partial x_i}(v-\varphi)=0, \qquad (38)$$

satisying the conditions

$$\lim_{x_2\to0}\frac{\partial v}{\partial x_2}=-\frac{1}{s\cosh(s\ell)}\ \text{ for}-1<x_1<1,$$

$$\lim_{x_2\to0}\left(\frac{\partial v}{\partial x_2}-\frac{\partial\varphi}{\partial x_2}\right)=-\frac{1}{s}\ \text{ for }-1<x_1<1,$$

$$\frac{\partial v}{\partial x_i} \to 0 \text{ and } \frac{\partial \varphi}{\partial x_i} \to 0 \text{ as } x_1^2 + x_2^2 \to \infty. \tag{39}$$

For solving (38) subject to (39), we take

$$v(x_1, x_2, s) = \text{Re} \int_0^\infty \{H(x_2)A(p,s)\exp(ip[x_1 + \tau(p,s)x_2]) - H(-x_2)A(p,s)\exp(-ip[x_1 + \tau(p,s)x_2])\}dp,$$

$$v(x_1, x_2, s) - \varphi(x_1, x_2, s) = \text{Re} \int_0^\infty \{H(x_2)B(p,s)\exp(ip[x_1 + ix_2]) - H(-x_2)B(p,s)\exp(-ip[x_1 + ix_2])\}dp, \tag{40}$$

where Re denotes the real part of a complex number, $H(x)$ is the unit-step Heaviside function, $\tau(p,s) = ip^{-1}\sqrt{p^2+s^2}$ and $A(p,s)$ and $B(p,s)$ are real functions yet to be determined.

It is easy to check that with (40) the far-field conditions given in the last line of (39) are satisfied and the partial derivatives $\partial v/\partial x_2$ and $\partial \varphi/\partial x_2$ are continuous on the plane $x_2 = 0$ which contains the crack.

To ensure that $v(x_1, x_2, s)$ and $\varphi(x_1, x_2, s)$ are continuous in the region $|x_1| > 1, x_2 = 0$, we take

$$A(p,s) = \frac{1}{\pi}\int_{-1}^{1} R(q,s)\cos(pq)\,dq,$$

$$B(p,s) = \frac{1}{\pi}\int_{-1}^{1} W(q,s)\cos(pq)\,dq, \tag{41}$$

where $R(q,s)$ and $W(q,s)$ can be shown to be to be related to the displacement jump Δu_3^* and the potential jump $\Delta\phi^*$ by

$$\left.\begin{aligned} R(q,s) &= \Delta u_3^*(q,s) \\ W(q,s) &= \Delta u_3^*(q,s) - \Delta\phi^*(q,s) \end{aligned}\right\} \text{ for } -1 < q < 1. \tag{42}$$

From (40), (41) and (42), the conditions on the first two lines of (39) give the hyper-singular integral equations

$$\frac{1}{\pi}\mathcal{H}\int_{-1}^{1}\frac{R(q,s)}{(q-x_1)^2}dq + \mathcal{C}\int_{-1}^{1} R(q,s)\Theta_0(q,x_1,s)dq + \int_{-1}^{1} R(q,s)\Theta_1(q,x_1,s)dq = -\frac{1}{s\cosh(s\ell)} \quad \text{for } -1 < x_1 < 1, \tag{43}$$

and

$$\frac{1}{\pi}\mathcal{H}\int_{-1}^{1}\frac{W(q,s)}{(q-x_1)^2}dq = -\frac{1}{s} \quad \text{for } -1 < x_1 < 1, \tag{44}$$

where

$$\Theta_0(q,x_1,s) = -\frac{s^2}{2\pi}\{\text{Shi}|q-x_1|\sinh|q-x_1| - \frac{1}{2}(\text{Ei}|q-x_1| - E_1|q-x_1|)\cosh|q-x_1|\},$$

$$\Theta_1(q,x_1,s) = -\frac{1}{\pi}\int_0^\infty [\sqrt{p^2+s^2} - p - \frac{ps^2}{2(p^2+1)}] \times \cos(px_1)\cos(pq)\,dp, \tag{45}$$

with $\text{Ei}(x)$ and $E_1(x)$ being the exponential integrals and $\text{Shi}(x)$ the hyperbolic sine integral defined in [1].

The hyper-singular integral equation in (44) can be easily inverted to obtain

$$W(q,s) = \frac{1}{s}\sqrt{1-q^2}, \tag{46}$$

which gives $\tilde{k}_{IV}^{+}(s) = 1/s$ and hence $K_{IV}^{+}(t) = 1$ for $t > 0$.

To solve (43) approximately, let

$$R(q,s) \cong \sqrt{1-q^2}\sum_{j=1}^{J}\omega_j(s)U_{j-1}(q), \tag{47}$$

where $\omega_j(s)$ are to be determined from

$$\sum_{j=1}^{J}\omega_j(s)\{-j\,U_{j-1}(w_i) + \Upsilon_j(w_i,s)\} = -\frac{1}{s\cosh(s\ell)} \quad \text{for } i = 1,2,\dots,J, \tag{48}$$

where

$$\Upsilon_j(w,s) = \mathcal{C}\int_{-1}^{1}\sqrt{1-q^2}\Theta_0(q,w,s)U_{j-1}(q)dq + \int_{-1}^{1}\sqrt{1-q^2}\Theta_1(q,w,s)U_{j-1}(q)dq. \tag{49}$$

Once $\omega_j(s)$ are determined from (48), $\tilde{k}_{III}^{\pm}(s)$ can be computed by

$$\tilde{k}_{III}^{\pm}(s) = -\frac{1}{s}e_{15} + \sum_{j=1}^{J}(1+e_{15})\,\omega_j(s)U_{j-1}(\pm 1), \tag{50}$$

and inverted to obtain $K_{III}^{\pm}(t)$ using (35).

10. Numerical results for specific problems

To test the validity of the numerical Green's function boundary element approach presented here, it is applied to solve the piezoelectric crack problem in Section 9 for a large ℓ. Specifically, we take $\ell = 20$.

Each side of the square domain is discretized into 40 equal length elements. For the approximations in (20) and (31), J is

taken to be 10, that is, 10 collocation points are employed on the crack to solve the hyper-singular integral equations (17), (18), (28), (29) and (43). To invert numerically the Laplace transform of of K_{III}^{+}, $P = 4$ is used in (35). The material constants for the piezoelectric material PZT-BaTio3 are chosen for the calculation. The non-dimensionalized e_{15} as defined below (6) is given by 0.2993.

In Fig. 2, numerical values of the stress intensity factor K_{III}^{+} computed from the boundary element solution are plotted against time t and compared with the values calculated from (50) which is derived from the semi-analytic Fourier transform solution. The two sets of values for K_{III}^{+} are in good agreement with each other.

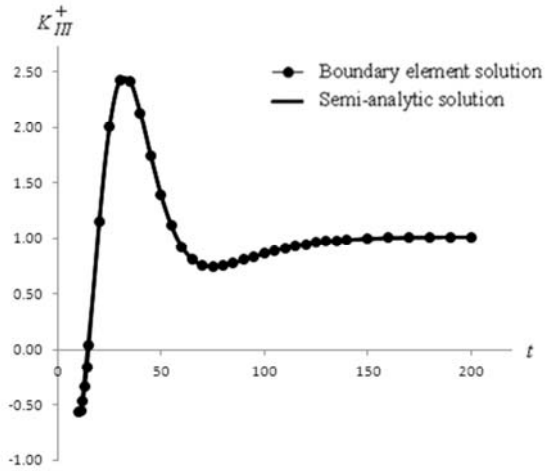

Figure 2: Plots of K_{III}^{+} against t

For another specific problem, consider now the case in which the electrically impermeable crack $-1 < x_1 < 1$, $x_2 = 0$, lies in the interior of the rectangular slab $-\ell < x_1 < \ell$, $-h < x_1 < h$, where ℓ and h are constants such that $\ell > 1$ and $h > 0$.

Parts of the exterior boundary of the rectangular slab are electroded such that

$$\phi(x_1, \pm h, t) = \pm H(t) \text{ for } d < x_1 < \ell,$$

$$\phi(x_1, \pm h, t) = \mp H(t) \text{ for } -\ell < x_1 < -d, \qquad (51)$$

where $2d$ is the gap between the two electrodes on each horizontal side of the slab. On the non-electroded parts of the boundary, the normal electrical displacement is zero. All the four sides of the slab are stress-free.

The sides of the rectangular slab are discretized into not more than 150 elements. As before, we take $e_{15} = 0.2993$ (that is, we take the piezoelectric material to be PZT-BaTio3) and use $J = 10$ and $P = 4$ in the numerical calculation.

For $\ell = 5.0$ and $d = 0.5$, the crack tip stress intensity factor K_{III}^{+} and electrical displacement intensity factor K_{IV}^{+} obtained by using the numerical Green's function boundary element procedure are plotted against t for $0.05 < t < 10$ in Fig. 3 and 4 respectively for selected values of h. As may be expected, the peak values of K_{III}^{+} and K_{IV}^{+} become larger as h decreases. Furthermore, as is visibly obvious in Fig. 3 and 4, K_{III}^{+} and K_{IV}^{+} attain their peak values at earlier times if h is smaller.

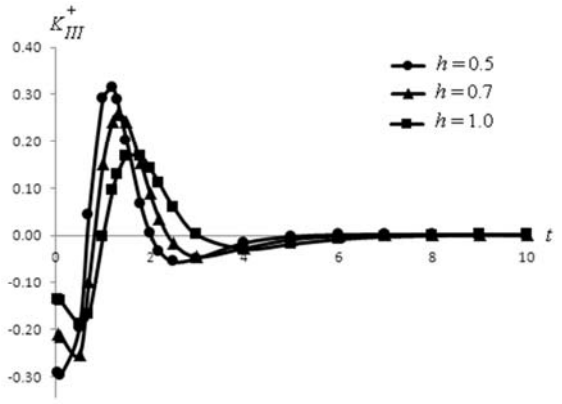

Figure 3: Influence of h on K_{III}^{+}

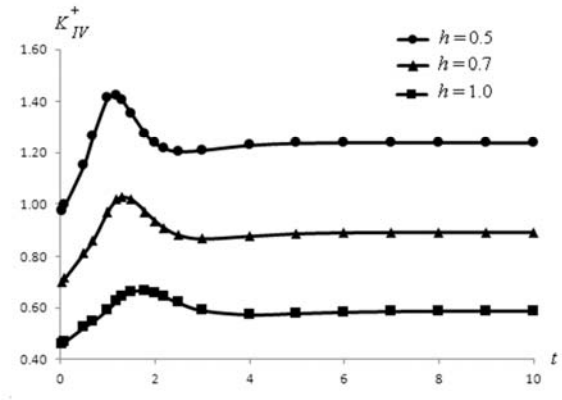

Figure 4: Influence of h on K_{IV}^{+}

Lastly, for $\ell = 5.0$ and $h = 0.5$, we examine the influence of the half-gap d between the two electrodes on each horizontal side of the slab on K_{III}^{+} and K_{IV}^{+}. From Fig. 5 and 6, it appears that decreasing d has the effect of increasing the peak values of K_{III}^{+} and K_{IV}^{+}. For $d = 2.0$, the magnitudes of K_{III}^{+} and K_{IV}^{+} are comparatively small.

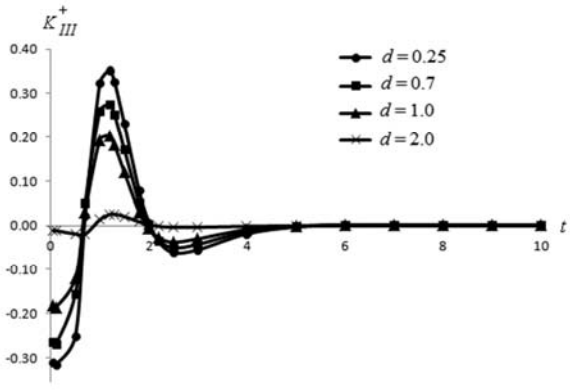

Figure 5: Influence of d on K_{III}^{+}

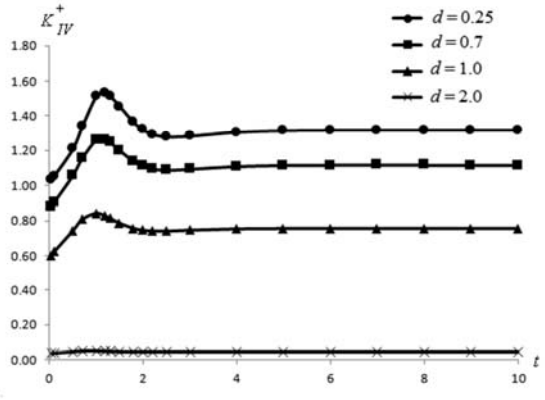

Figure 6: Influence of d on K_{IV}^{+}

11. Summary and final remark

Green's functions are constructed numerically in the Laplace transform space for an electrically impermeable planar crack in an infinite piezoelectric solid undergoing an anti-plane dynamic deformation. We apply the Green's functions to derive a simple boundary element method for solving numerically anti-plane dynamic piezoelectric crack problems involving finite solution domains. The boundary element procedure requires only the exterior boundary of the solution domain to be discretized into boundary elements, that is, no discretization of the crack faces is needed. For a special case of the problem, the boundary element solution is verified using a semi-analytic Fourier integral transform solution. The analysis presented here for deriving the numerical Green's functions can be readily extended to multiple planar cracks and curved cracks.

References

[1] Abramowitz, M. and Stegun, I.A., *Handbook of Mathematical Functions*, Dover, New York, 1971.

[2] Ang, W.T., A boundary integral equation for deformations of an elastic body with an arc crack, *Quart. Applied Maths*, 45, pp. 131-139, 1987.

[3] Ang, W.T. and Clements, D. L., A boundary integral equation method for the solution of a class of crack problems, *J. Elast.*, 17, pp. 9-21, 1987.

[4] Ang, W.T. and Telles, J.C.F., A numerical Green's function for multiple cracks in anisotropic bodies, *J. Engng Maths*, 49, pp. 197-207, 2004.

[5] Athanasius, L., Ang, W.T. and Sridhar I., Numerical Green's functions for some electroelastic crack problems, *Engng Analysis with Boundary Elements*, 33, pp. 778-788, 2009.

[6] Clements, D.L. and Haselgrove, M.D., A boundary integral equation method for a class of crack problems in anisotropic elasticity, *Int. J. Computer Maths*, 12, pp. 267-278, 1983.

[7] Kaya, A.C. and Erdogan, F., On the solution of integral equations with strongly singular kernels, *Quart. Applied Maths*, 45, pp. 105-122, 1987.

[8] Snyder, M.D. and Cruse, T.A., Boundary integral analysis of cracked anisotropic plates, *Int. J. Fracture*, 11, pp. 315-328, 1975.

[9] Stehfest, H., Numerical inversion of the Laplace transform, *Comm. ACM*, 13, pp. 47-49 (see also p. 624), 1970.

[10] Telles, J.C.F., Castor, G.S. and Guimaraes, S., A numerical Green's function approach for boundary elements applied to fracture mechanics, *Int. J. Num. Meth. Engng*, 38, pp. 3259-3274, 1995.